Parametric Analysis of The Effect of CRS Seatback Angle in Dummy Measurements in Frontal Impacts.

Manuel Valdano, Juan M. Asensio-Gil, Jesús R. Jiménez-Octavio, Miguel Cabello-Reyes, Rodrigo Vasserot-Tolmos, Francisco J. López-Valdés

Abstract The objective of this study was to assess the effect of modifying the seatback angle of a Child Restraint System (CRS) in the dummy readings and in the associated injury criteria in frontal impacts, performed according to the specifications of the regulation UN R129. A multibody model of a CRS was developed and validated using the experimental results obtained in a frontal impact of a commercial rear-facing infant seat (45-86 cm) using the Q1.5 dummy. Then, the seatback angle of the CRS was virtually modified in the multibody model of the CRS between +10 degrees (more vertical) and -10 degrees (more horizontal) at 2.5 degrees intervals. The average CORA rating resulted on a fair score (0.611 average rating) of the dummy readings. The modification of the seatback angle showed that there is a trade-off between the forces and moments acting on the cervical and the lumbar areas of the spine. Although a more vertical configuration resulted in an improvement of the criteria specified by the regulations (average 15% reduction using +10 degrees), spine loads resulted on values three times higher than the reference configuration. Further research is needed to assess if the lumbar spine loads may reach injurious levels for these reclined postures.

Keywords Child restraint system, CRS, multibody model, neck injuries, spine injuries

I. INTRODUCTION

In 2018, between 1.9% and 2.25% of global deaths and between 2.6% and 3.04% of global disability-adjusted life years (DALYs) were related to road traffic injuries [1], amounting to 1.2 million deaths. The World Health Organization (WHO) [2] estimated that around 29.0% of these deaths corresponded to vehicle occupants. If the focus is on younger victims, road traffic injuries are the leading cause of death for children and young adults between 5 and 29 years old globally and the second one for children between 1 and 4 years old in high-income countries [1]. At the global scale, almost 40% of all paediatric deaths between 0 and 9 years old corresponded to vehicle occupants.

Child Restraint Systems (CRS) have been shown to be extremely effective in the prevention of paediatric injuries, reducing the probability of sustaining severe injuries by 64% and the risk of death by 71% [3]**.** The effect of using a CRS in young children has been compared to the effect of using the seatbelt to prevent death in adult occupants [4]**.** There are different CRS types available on the market, whose classification in different categories varies among associations or countries. For instance, the United Nations Regulation No. 129 (UN R129) [5] classifies child seats according to three characteristics: the type of CRS (integral or non-integral), how the CRS is attached to the vehicle (using the ISOFIX anchorage or the vehicle seatbelt) and the positions in which the CRS can be installed in the vehicle (i-Size or specific vehicle). In addition, each CRS manufacturer determines which is the appropriate user's height range for a particular CRS. This regulation also establishes that under 15 months old all CRS must be rear-facing.

One of the key parameters in infant car seat design is the seatback angle, which affects both child safety, its comfort and the quality of the necessary sleep in the case of younger children. In terms of child safety in rear facing CRS, previous studies have analyzed the influence of modifying the recline angle of the CRS in the upper cervical spine [6]. But, a variation in the seatback angle has an influence on the overall kinematics and dynamics of the child, and therefore could have an effect on the risk of injury to the head, neck, thorax and lumbar spinal regions. At the same time, specialised literature has suggested that children aged 0 to 3 years old may need up to 16 hours of uninterrupted sleep (8 of which happen during daytime) [7], preferably on a flat and firm surface [8]. As a result of this recommendation, infant seats attempt to provide a position as reclined as possible while

M. Valdano (+34 644 64 05 53, mvaldano@comillas.edu) is a PhD. student, J. M. Asensio-Gil and R. Vasserot-Tolmos are MSc. students, J. R. Jiménez-Octavio is a Professor and Researcher, M. Cabello-Reyes is a MSc., and F. J. López-Valdés is an Associate Professor and Researcher at Instituto de Investigación Tecnológica (IIT), ICAI, Universidad Pontificia Comillas, Madrid, Spain.

keeping the appropriate level of protection for the paediatric occupants. A recent review of the literature addressing potential breathing issues in neonates found that semi-upright child seats could contribute to the obstruction to the airways due to the lack of cervical muscle tone that would facilitate the flexion of the head [9] This risk could be of special concern in preterm and low birth weight infants. However, this review also recommends a frequent follow up of these children so that they transition to an upright child seat as soon as it is possible and the risk for airways obstruction is minimal. To date, it is not clear which would be the optimised seatback angle that can ensure optimal protection to the child without compromising breathing and providing an acceptable comfort level to the infant [10]. Given the consequences that modifying the CRS seatback angle may have in the overall health of children, understanding the implications of varying this parameter in the injury likelihood in case of impact may contribute to provide design guidelines for CRS, which will need to consider also the other aspects of child health aforementioned.

Thus, the aim of this study was to assess the effect of modifying the seatback angle of a rear facing CRS in the dummy readings and in the corresponding injury criteria in frontal impacts, performed according to the specifications of regulation UN R-129. seatback

II. METHODS

A multibody model of a CRS was developed using Simcenter Madymo™ (Helmond, Netherlands). The model was validated using experimental results obtained in a frontal impact of a commercially available rear-facing infant seat (40-86 cm). This experiment was performed with the Q1.5 dummy and according to the specifications of regulation UN R-129. The validation of the model was performed by direct comparison of the kinematics of the CRS and a Correlation and Analysis (CORA) of the dummy readings. Once the baseline model was validated, the seatback angle of the CRS was modified virtually in the multibody model of the CRS ranging between -10 degrees from the baseline (more horizontal) and +10 degrees from the baseline (more vertical) at 2.5-degree intervals.

Computational Model of the UN R-129 Test Bench and Test Setup

The geometry of the UN R-129 test fixture was simplified from a CAD version of the bench. The original anchoring points of the UN R-129 were maintained in the same position and modelled as rigid bodies, and a non-pre-tensioned, non-force-limited seatbelt was used. The seatbelt webbing had a constant width of 50mm and a tension of 20kN at 10% elongation. Fig. 2 shows a section of the model used to carry out the simulations.

A key component affecting the response of the model was the interaction between the CRS and the seat surface and the seatback rest of the test bench. These two seat surfaces were modeled with a planar surface and a hyper-ellipsoid for the seatpan and seatback, respectively. To adjust the contact characteristics between the CRS and the test bench in the multibody model, a finite element (FE) model of the test bench was also developed in LS-Dyna. The force-penetration curve required to define the contact characteristic in Madymo was obtained in an iterative process consisting of the following steps:

i. The adjustment of the material properties of the FE model of the foam using the experimental data obtained from the calibration test of the seat cushion as described in UN R-129 (see Fig. 1).
ii. Once the response of the test bench model matched the experimental results in the calibration tests, a FE model of the bottom part of the CRS was used to load the seat surface and obtained the force vs. penetration functions for the contact between the two parts.
iii. A damping model was calculated based on the functions obtained in the previous step.

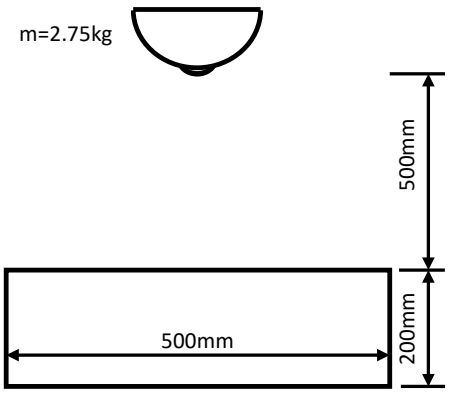

Fig. 1. Illustration of the experimental setup used to test the foam according to the UN R-129 regulation.

The foam definition in the FE model used a Fu Chang material property for the seatpan, which was adjusted to match the experimental test results using the acceleration measured at the impactor. In the effort of adjusting the contact definition for the multibody model, the FE simulations involving the bottom part of the CRS and the test bench were performed at a wide range of prescribed penetration velocities (ranging from 0.014 m/s to 14 m/s) to obtain a comprehensive range of loading conditions of the foam. The contact force with the 0.014m/s penetration velocity was taken as a quasi-static test and the damping coefficient required in the definition of the contact function in Madymo was calculated using the equation:

$$\boldsymbol{F_{c(d,v)} = F_{0(d)} + v\, c_{(v)}\, F_{0(d)},} \quad (1)$$

where $F_{c(d,v)}$ is the contact force for a given penetration (d) and penetration rate (v), $F_{0(d)}$ is the contact force for a given a penetration in a quasi-static test and $c_{(v)}$ is the damping coefficient, which is a function of the penetration rate. The damping coefficient was calculated for penetrations between 20 and 50mm, which were then used to calculate the mean damping coefficient to be used in the multibody model.

Computational Model of the CRS

The geometry of the CRS model was obtained directly from the CAD model of the tested CRS. Its inertial properties were adjusted to match the mass and inertia of the actual CRS (m=2.44kg) by splitting the physical CRS into its different components. The model consisted of four elements: a rigid CRS structure (shell elements), a rigid headrest padding (shell elements), one rigid surface representing the internal foam of the seatpan and one rigid surface representing the internal foam of the backrest (Fig. 3). The deformable properties of the previous components were modeled by the definition of contact functions between these surfaces and the corresponding ones in the Anthropomorphic Test Device (ATD) model. The CRS model also included a three-point belt harness used to restrain the occupant. The width of the CRS three-point harness was 20mm and its tension properties were obtained scaling the test bench seatbelt. Three spring elements were used to tighten the CRS harness (using an initial tension of 7N) during the positioning process. The springs were blocked after the fastening process to keep the initial tension constant at the beginning of the test. The contact characteristics of the ATD and internal padding components were adjusted during the validation process.

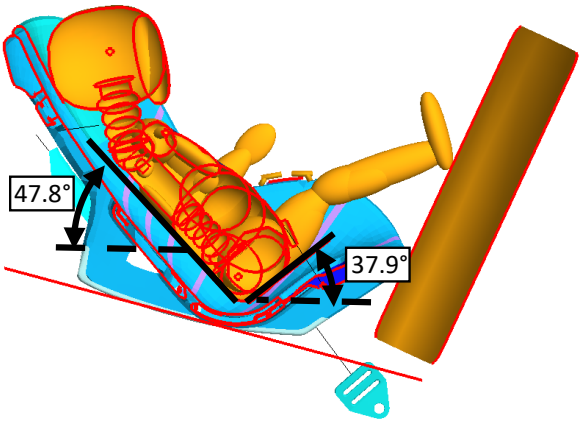

Fig. 2. Sagittal section of the CRS, ATD and test bench models used in the study. Angles of the seatback and seatpan with the horizontal plane in the baseline model.

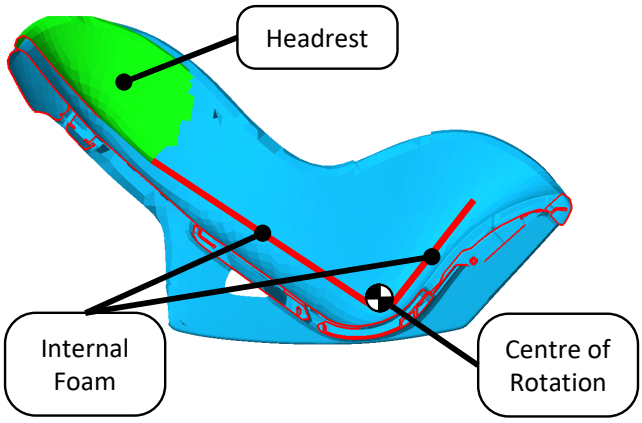

Fig. 3. Detailed section of the CRS, identifying the inner contact surfaces with the ATD and the center of rotation used to modify the seatback angle.

Experimental Test and Validation of the Multibody Model

The multibody model was benchmarked against experimental data obtained in a frontal-impact test carried out according to the UN R-129 procedure. The experimental acceleration pulse for the 52 km/h impact measured in the sled is shown in Fig. 4. The shadowed area shows the acceleration corridor specified in the regulation. The experimental test available to validate the multibody model was performed with the Q1.5 ATD model.
The model of the CRS and the Madymo model of the Q1.5 dummy [11] were allowed to settle on the test bench using gravity. To this end, the Madymo simulations were 550ms long: the first 400ms were required to position the CRS and ATD models on the test bench and tighten the sled seatbelts, while the remaining 150ms were

employed to prescribe the acceleration pulse of the frontal crash to the test bench. Fig. 5 shows the computer model after the positioning process.

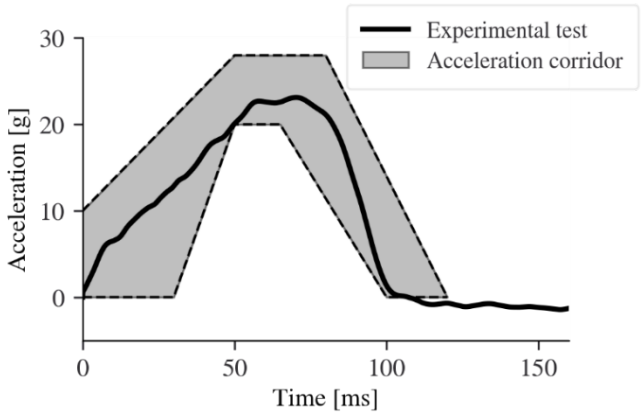

Fig. 4. Crash acceleration pulse measured at the sled and corridor specified in the UN R-129 regulation for the homologation frontal-crash test.

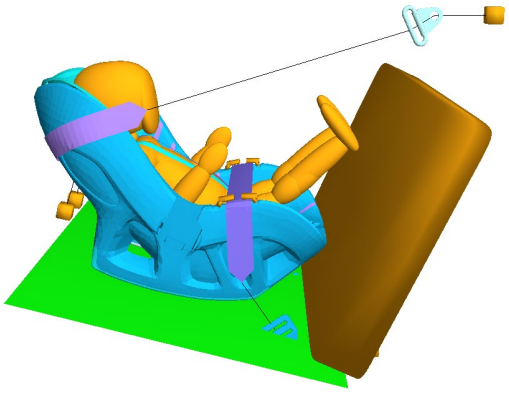

Fig. 5. Computer model after the positioning process.

The CORA method [12-13] was used to validate the response of the model using 11 dummy readings: the linear acceleration of the head in the X, Y, and Z axes; the axial force measured in the upper neck load cell; the moments in the X, Y, and Z axes measured in the upper neck loadcell; the linear acceleration of the thorax in the X, Y, and Z axes; and the chest deflection. These signals were measured at 10kHz and then filtered following the standard SAE J211 [14]. The same weight was applied to each signal to obtain the average rating of the model. The corridors used to rate the response were generated using 5% and 20% of the peak signal value for the inner and outer corridor, respectively. The weights used to combine the rating methods for each signal were 0.5 for the corridor method, 0.25 for the cross-correlation method, 0.125 for the size method, and 0.125 for the phase shift method. The time window used in the rating process began with the application of the acceleration pulse and ended after 150ms, which was enough to consider all peak values in the time window analysed. The ratings were categorised using the ISO/TR 9790:1999 biofidelity scale, which defines: excellent rating (8.6 ≤ rating ≤ 10.0); good rating (6.5 ≤ rating < 8.6); fair rating (4.4 ≤ rating < 6.5); marginal rating (2.6 ≤ rating < 4.4); and unacceptable rating (0.0 ≤ rating < 2.6).

Changing the Seatback Angle of a Child Restraint System (CRS) and Quantitative Assessment of the Response

After the validation of the original CRS, the seatback angle of the system was modified in the computational model by rotating the mesh nodes of the seatback between -10° and 10° at 2.5° intervals. These modifications of the CRS structure were performed in LS-PrePost. The moment of inertia of each configuration was recalculated based on the new mass distribution obtained from the finite element model. Then, each model was translated to Madymo. Fig. 6 shows the configuration of the CRS models with the modification in the seatback angle.

To ensure a similar relative position of the paediatric dummy and the CRS, the relative position between the ATD pelvis and a reference point in the seat surface of the CRS was controlled across all the seatback variations. The maximum difference in this relative position of the ATD h-point was 2.79mm (1.38 mm, average). The rotation of the CRS was also computed to observe the impact of restraining the CRS using the seatbelt on the CRS orientation at the beginning the acceleration pulse. This process used the orientation of the seatpan, which was not modified in the generation of the different geometries, to compute the orientation of the CRS. The largest angle between seatpans measured between two given models was 0.3°, which was observed when the more upright and more reclined positions of the seatback were used.

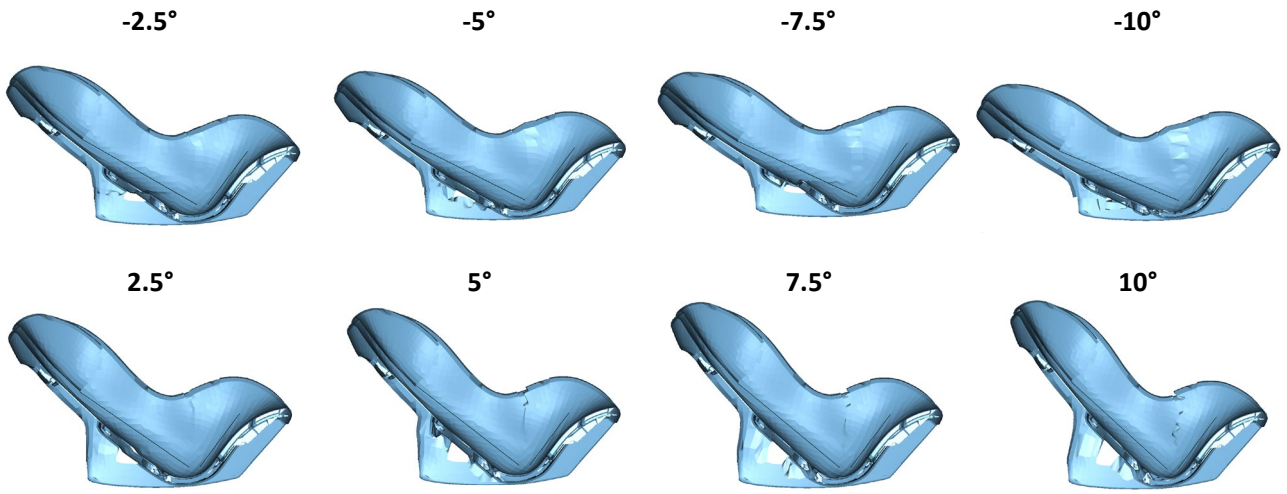

Fig. 6. Modifications in the seatback angle between -10° and 10° from the original CRS model.

In the assessment of the effect of changing the seatback angle of the CRS on the child ATD responses, the peak values of the following signals were considered: *i*) head acceleration (3ms); *ii*) thoracic acceleration (3ms); *ii*) neck tension force; *iv*) neck compression force; *vi* neck shearing force; *v*) neck extension moment; *vi*) neck flexion moment; *vii*) lumbar tension force; *viii*) lumbar compression force; *ix*) lumbar shearing force; *x*) lumbar extension moment; and *xi*) lumbar flexion moment. A set of injury criterion thresholds were compared to the variations in the injury criteria mentioned above. TABLE I shows these thresholds for an 18-month infant, which were based on the injury assessment reference values (IARV) proposed by [15] for the CRABI and Hybrid III families of child dummies; and the UN R-129 regulation [5] with limits for the Q1.5 dummy, which also included the neck limits of the regulation proposal for the 04 series of amendments [16-17]. There is a difference between the criteria used for the maximum head acceleration between the two references, as the former uses the peak value of the signal and the latter uses the 3ms criteria. Even if the criteria proposed by Mertz are applicable to a different family of dummies, these IARV were considered relevant for this study if only as a qualitative reference.

TABLE I
Injury criterion thresholds for an 18 Month Infant

Criteria	Thresholds	
	Mertz	UN R-129
Head acceleration	160g	75g
Thorax acceleration	55g	55g
Neck tension force	1080N	950N
Neck compression force	1040N	-
Neck shear force	810N	-
Neck extension moment	15Nm	-
Neck flexion moment	29Nm	30Nm
Neck lateral moment	22Nm	-
Neck twist moment	15Nm	-

III. RESULTS

Development and Validation of the Computer Model

As aforementioned, the quality of the response of the multibody model (test bench+CRS+Q1.5) was assessed using the CORA method. The average CORA rating for the dummy readings was 0.610, which jointly with the kinematic comparison with the CRS displacement and rotation, was considered a valid approximation of the experimental model. TABL II shows the rating for each dummy reading included in the validation. The time history of all dummy readings for the simulation and experiment can be seen in Fig. 11 in the Appendix. Fig. 7 shows a series of snapshots in 30ms intervals of the simulated tests. There was neither a linear nor rotational accelerometer placed at the CRS to assess the dynamic response of the CRS, and therefore the kinematics of the CRS model could be only assessed by visual inspection.

As shown in TABLE II, most of the signals used in the validation of the model received a good rating in the CORA assessment. Two signals received a fair rating while three of them were ranked as marginal (head acceleration in the Z axis, neck tension force, and thoracic acceleration in the Y axis).

Head acceleration in the Z axis and neck tension force were, of course, highly correlated. Although different attempts were made to increase the CORA ratings for these two signals by modifying the contact characteristics between the head and the CRS (friction, damping, magnitude of the contact force), the solution provided here was the one that better represented the experimental results. A close look at the time history plots included in the Appendix, shows that the simulated response of the neck tension force was similar in magnitude and phasing (although there was a slight delay in the peak tension force) to the one measured in the experiments, despite its oscillations and that, at times, the simulated curve did not stay within the CORA corridor. The head acceleration in the Z axis did not match correctly the acceleration measured by the physical ATD from t=55ms. However, the modifications of the contact characteristics to improve the Z head acceleration component resulted in worse results for the neck tension force, which was very sensitive to the characteristics of the contact between the ATD head and the padding (higher friction coefficients resulted in high compression neck forces; lower friction coefficients resulted in large tension neck forces). Thus, the solution included here was considered an acceptable trade-off.

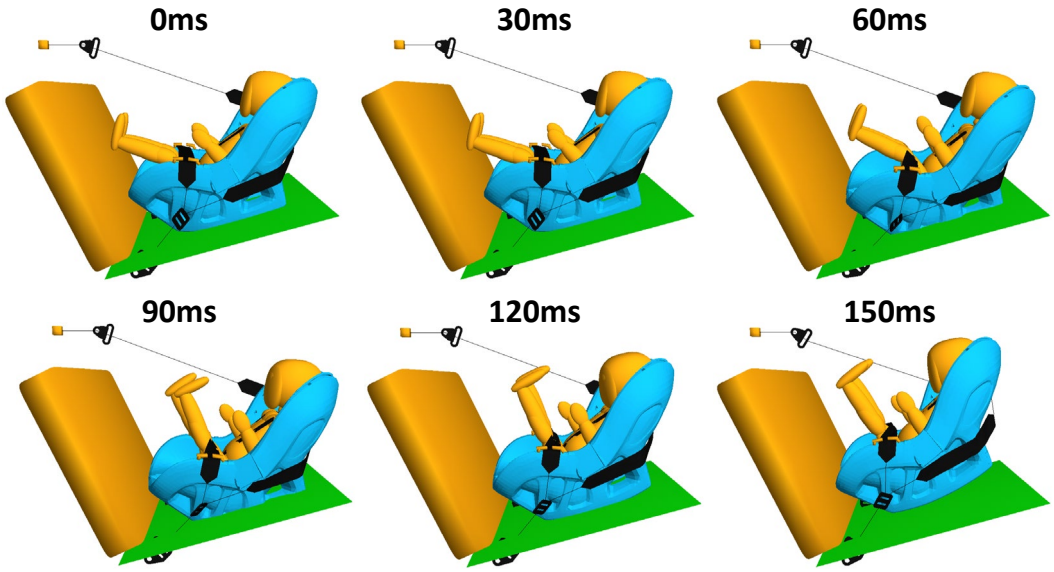

Fig. 7. Snapshots of the frontal-crash test simulation used for the model validation each 30ms.

As for the thoracic acceleration in the Y axis, its magnitude was almost five times lower than the other two components, that received a good score in the CORA assessment. Given that the test scenario being simulated was a frontal impact, it was considered that this deviation in the simulated lateral component of the thorax acceleration was acceptable.

TABLE II
CORA RATING OF THE MODEL PREDICTIONS

Signal	Rating	Assessment
Head acceleration X	0.817	Good
Head acceleration Y	0.694	Good
Head acceleration Z	0.399	Marginal
Neck tension force	0.356	Marginal
Neck moment X	0.809	Good
Neck moment Y	0.540	Fair
Neck moment Z	0.690	Good
Thorax acceleration X	0.858	Good
Thorax acceleration Y	0.442	Marginal
Thorax acceleration Z	0.693	Good
Thoracic compression	0.418	Fair
Average	0.611	Fair

It needs to be pointed out that experimental measurements of the initial position of the ATD within the CRS were not available and the positioning of the model was made by visual comparison with the high-speed video images (Fig. 8). Most likely, a more detailed description of the initial position of the dummy would have impacted positively some of the signals that were rated as marginal.

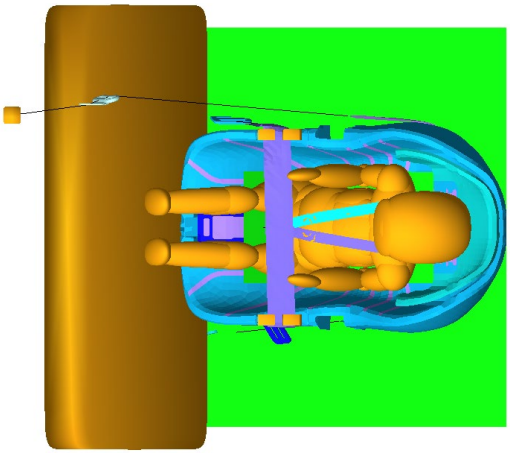

Fig. 8. Top view of the multibody model after the positioning process.

Assessment of the Model Response for Changing the Seatback Angle of the Child Restraint System (CRS)

Eight CRS models were developed by modifying the seatback angle of the CRS shown in the previous section. The variation of the seatback angle was from -10° (more horizontal) to +10° (more vertical) at 2.5° intervals. TABLE III shows the values obtained for the injury criteria considered in this study for the baseline case (unmodified model, validated as shown in the previous subsection and labelled as 0°), and the differences in percentage obtained when the angle of the seatback was increased or decreased.

TABLE III

Injury criteria readings variation in relation to the dummy reading in the reference simulation (0°).

Backrest Angle	-10°	-7.5°	-5°	-2.5°	0°	2.5°	5°	7.5°	10°
Head 3ms	+9%	+9%	+6%	+5%	31.1g	-9%	-7%	-13%	-9%
Thorax 3ms	+7%	+8%	+5%	0%	32.0g	-8%	-4%	-3%	-7%
Neck +Fz	+94%	+60%	+20%	+3%	113N	+24%	+49%	+46%	+52%
Neck -Fz	-67%	-52%	-65%	-16%	112N	+25%	+30%	+41%	+106%
Neck Fx	-2%	-2%	+3%	-2%	535N	-4%	-8%	-13%	-13%
Neck -My	-1%	-4%	0%	-7%	27.2Nm	-15%	-13%	-19%	-22%
Neck +My	+5%	-5%	+5%	-7%	6.98Nm	+9%	-12%	-5%	-10%
Neck Mx	+19%	+7%	+16%	+2%	7Nm	-9%	1%	-2%	-14%
Neck Mz	+6%	-3%	+8%	-22%	10.6Nm	-10%	-7%	-6%	-4%
Lumbar +Fz	-35%	-30%	-39%	-33%	72N	+254%	+150%	+150%	-19%
Lumbar -Fz	+55%	+56%	+31%	+19%	243N	+4%	+48%	+58%	+91%
Lumbar Fx	-2%	+4%	-2%	+10%	237N	-9%	+195%	+168%	+152%
Lumbar +My	-4%	+6%	-4%	-10%	11.9Nm	-15%	+193%	+178%	+192%

+Fz: Tension force
-Fz: Compression force
+My: Flexion moment
-My: Flexion moment

Not all the injury criteria included in this assessment are required in UN R-129. All dummy values specified at the regulation UN R-129 were far from reaching their thresholds. In general, the values limited in UN R-129 for all the seatback configurations remained around a 25% of the regulation proposed threshold. It was the thoracic acceleration that reached a value that was 62% of the threshold in the -7.5° horizontal seatback position.

A different observation was made for some of the injury criteria related to the cervical area. The injury criterion threshold proposed in [15] was exceeded by the neck extension moment (between 41% and 81% depending on the seatback angle). It should be noted that even in the unmodified original CRS these values were also over the proposed thresholds .

The time history plots of the neck loads are shown in Figure 9. The neck axial forces showed a transition from “always in tension” when a more reclined position of the seatback angle was used (-10°) to “always in compression” when a more upright position was used (+10°). Regardless of the direction of the axial force, both cases presented similar peak values around 200N. The bending moment behavior was different from that of the axial force, as all simulations showed similar tendencies. For this load, a more upright position reduced up to 22% the peak values in relation to the nominal one.

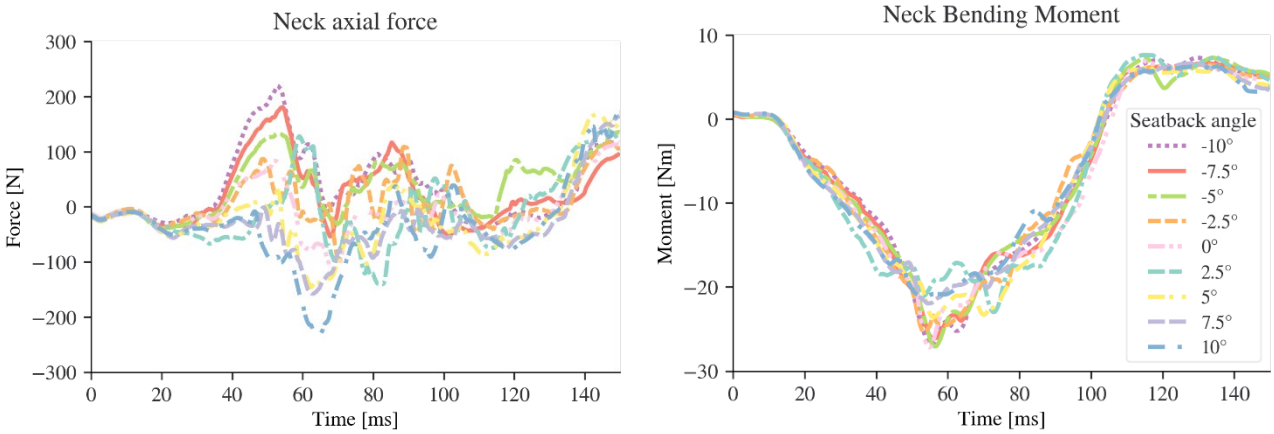

Fig. 9. Neck axial force (left hand side figure) and bending moment (right hand side figure) for a CRS with the seatback angle between -10° and 10°.

The large increment in lumbar loading with increasing seatback angle reached up to more than 250% of the values observed in the baseline condition. This increment can be explained by the kinematics of the dummy lower extremities in the vertical configurations (positive seatback angles), which resulted in the knees moving towards the dummy chest. The large values of the lumbar load cell were associated to large rotations of the dummy pelvis.

Fig. 10 shows the time history of the lumbar spine bending moment observed in the simulations for the different seatback angles (flexion values are positive; extension values are negative). Positive rotations of the seatback angle resulted in peak flexion moments occurring around 50ms, which were not observed for the rest of configurations. These peaks occurred before the ATD legs contacted the lap belt of the test bench, and therefore it was hypothesised that the lack of interaction of the thighs with the lap belt could lead to larger pelvic rotations and increase the lumbar loads. To verify this hypothesis, a simplified simulation isolating the ATD and imposing a rotation of the legs was performed, showing a stiffening effect of the lumbar joint similar to the observations from the simulations for comparable rotation angles. Thus, this numeric result should be taken with caution as it can be associated with a potential limitation of the model.

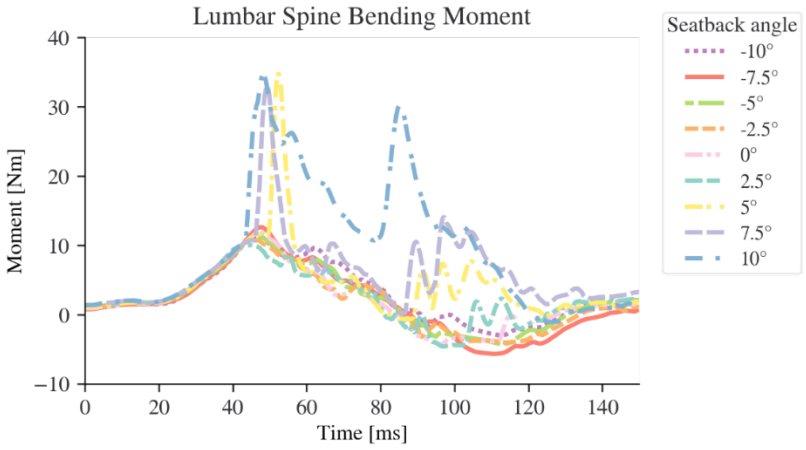

Fig. 10. Spine bending moment for a CRS with the seatback angle between -10° and 10°.

Seven of the thirteen analysed injury criteria showed a decrement with increasing the seatback angle (more vertical configuration). These injury criteria were: the head acceleration (3ms); the thoracic acceleration (3ms); the neck shear force; and all neck moments. The most relevant change observed with more vertical positions is the 22% reduction in the neck extension moment, especially since this value was larger than the injury criterion

thresholds proposed in [15] even in the baseline configuration. However, this modification also resulted in a large increment of lumbar loading, which reached magnitudes 2-3 times larger than the ones observed for the base model.

IV. DISCUSSION

The scope of this study was to provide guidance for CRS design by developing a multibody model of a system and testing different seatback angle configurations. The computational approach using multibody modelling of such modification provides an efficient tool to analyse the implications for the protection of paediatric occupants. Other studies using multibody simulations have been used before to optimise dummy readings in frontal impacts with high back booster seats [18], but this is the first one that analyses the influence of the seatback angle in infant seats.

The CORA rating method was used to assess the model fidelity, which resulted in an overall fair rating (0.61). Although three signals were ranked as marginal and two others as fair, these signals are not the most relevant ones in the assessment of the protection provided by the CRS and their relative contribution to the overall CORA rating could have been reduced. The signals with a marginal rating were the head acceleration in the Z axis, the neck tension force and the thoracic acceleration in the Y axis. The two first are closely related, and therefore the used approach doubled the penalty for a bad rating of the head acceleration in the Z axis. This signal showed similar values in the simulation as the ones observed in the experiment up to a time of 50ms, after this time window a sudden drop of the Z acceleration component was observed while the experimental curve continued increasing (Figure 11). Despite these differences in head acceleration, the visual comparison of the neck axial force provided a good match between the experimental and the simulation results for the whole duration of the experiment. None of the parameter combinations used in the contact definition of the head and the CRS was able to improve the prediction of the reference acceleration signal. This difference could be attributed to two factors in the model. First, it could have been caused by the approximation of the initial position of the model for the CRS, seatbelt, and child ADT. Although a set of pictures was used to visually match the initial position of the models, more accurate data were not available. Secondly, the marginal rating obtained for the neck tension force was the result of a difference in phase between the signals as both of them were oscillating (Figure 11). Therefore, the current approach using the CORA method to rate this signal was over-penalising these differences in phase.

The thoracic acceleration in the Y axis also had a marginal rating. The peak value observed for this signal was one fourth of the peak value observed for the thoracic acceleration in the X axis. Thus, a different weighting approach in CORA could have been implemented to have larger weights in those signals that have higher relevance for the validation; as in [19], which proposed a calculation of the weights based on the peak values for a group of signals. The application of this approach would result in the following normalised weights for the validation performed in this study: 0.50, 0.12, and 0.38 for the thoracic accelerations in the X, Y, and Z axes, respectively. This suggests that the lateral acceleration would have had approximately one tenth of significance in the prediction of the thoracic acceleration validation.

Regarding the fair ratings, these were observed for the thorax deflection and the neck bending moment. No special attention was given to the first one as it had a peak value of 1 mm, which is far from the minimum threshold (21 mm) proposed by [15] by scaling the injury criterion for an 18-month old child. As for the neck bending moment, although its peak value was 26.5Nm and 27.2Nm for the experiment and the simulation, respectively, the peak of the simulation was ahead of the experiment by 25ms. This difference was likely the result of the difference in the head acceleration for the Z axis, as the thorax continued its upward displacement resulting in the loading of the neck. It was found that the time for the Z axis head acceleration drop matched the peak loads for the neck shear force and bending moment. Despite these differences, it was decided that the overall fidelity of the model was good enough to carry out the rest of the study.

Then, the CRS model was modified into eight different configurations by changing the seatback angle. These modifications impacted on the injury criteria differently. Most of the criteria sustained a variation lower than ±30% with respect to the baseline case. However, spinal loads and neck forces showed larger variations, which were as much as +254% for the lumbar spine tension force.

The increment of the seatback angle (a more vertical configuration) resulted in a reduction of all injury criteria considered for the regulation [5], which included the head, neck, and thoracic criteria. This reduction is especially important for the neck moment extension criteria, as the criterion exceeded the limit in [15] even for the baseline

case. However, these limits were developed for the CRABI and Hybrid II families of child dummies, and therefore the repercussion of these measures on the injuries in the real world is not clear.

It should be noted that the improvement in the neck values came at the cost of increasing the lumbar loads as much as 250%, so this effect deserves further investigation. However, this result must be taken with caution as the simulated lumbar loads could not be benchmarked against experimental data. In parallel, an injury criterion for the paediatric lumbar spine that could help to weigh the improvement or worsening of the occupant safety does not exist, which hinders drafting conclusions applicable to the actual protection of children in the real world from this finding. Our recommendation is to continue exploring the possible implications of such configurations in the spine to avoided possible undesired outcomes (i.e., a surge in lumbar spine injuries with a reduction of neck injuries). It was hypothesised that the surge in spine loads was the result of the high rotation in the hip joints, which impacted the spine loads due to a hardening of the joint restraint. The analysis of the model in a more controlled environment showed the same pattern, as the one observed in the simulations of the CRS, confirming the hypothesis. An analysis of the response using the physical child ATD will clarify if this may be observed in the physical model or if it is related to the computer model working outside of the validated setups.

Although the restraint used for the CRS in this study and in reference [6] are different (restrained with the bench belt vs restrained with an ISOFIX base), the seatback angle measured from the horizontal plane had similar values (47.8° vs 47°, respectively). Thus, the predictions between both studies were contrasted when possible. In [6], the variation in the seatback angle was only ±5°. In the present study, the load observed in the dummy for the were around 50% of the ones observed in [6] for the same angle variation in six out of the seven dummy signals. These signals could be categorized into accelerations and neck loads: the first one contains the head and thoracic acceleration and the latter contains the axial and shearing forces and the flexion bending moment at the neck. The acceleration at the head showed a 10g difference between the measures in this study vs the cited one (ranges: 27-34g vs 45-60g, respectively), but the thoracic accelerations showed a smaller difference (ranges: 30-35g vs 35-43g, respectively). Neck loads showed three different behaviors: lower axial forces with 37-230N vs 210-265N, respectively, for compression loads and 110-200N vs 470-880N, respectively, for traction forces; similar flexion bending moments with 6.1-7.6Nm vs 6.6-9.2Nm, respectively; and higher shearing forces with 470-550N vs 280-340N, respectively. All of the observed loads and accelerations in both studies were below the current and proposed limits in the regulation. One of the cases in the cited study contacted the steel tube, which was not observed in this study. While, the head displacements for the setups in the cited study ranged from 153-192mm, in the current study they ranged from 42-62mm. Figure 12 at the appendix shows the head displacements for the simulated configurations.

The main limitation of this study was the limited number of impact conditions included. Firstly, it was considered only the frontal impact for the approval test of the regulation UN R-129 using a commercial CRS. Furthermore, the simulations were carried out with the Q1.5, while the type approval test would also include the use of the ATD Q0. Although the modification of the seatback angle may mainly impact the results on frontal impacts, this modification may also modify the interaction between the CRS and the sled seatbelt system due to the differences in the seatbelt routing. Secondly, the CRS was restrained with the sled seatbelt system, instead of a base fixed to the sled using the ISOFIX mechanism, in an attempt to examine a worst-case scenario. Another relevant consideration is that some of the differences identified in the study could be within the typical ranges of repeatability of the Q-series dummies. Unfortunately, the experimental data that were used in the development of the baseline model were from just one test and it was not possible to include the effect of experimental variability in the assessment of the results presented here

V. CONCLUSIONS

A simplified multibody model of a commercial CRS was developed and benchmarked against experimental data from frontal impacts. The model was used to understand how several dummy readings changed when the seatback angle of the CRS was modified. The results showed that there was a trade-off between the forces and moments acting on the cervical and the lumbar areas of the spine. Although more vertical seatback angles resulted in the improvement of the criteria specified by the regulations, they also resulted in lumbar spine loads as high as three times the reference one. Thus, it would be necessary to further study the possible implications of the surge of these loads to avoid undesired outcomes and to weigh the possible improvement and worsening of different solutions on the measured injury criteria.

VI. REFERENCES

[1] "GBD Results Tool | GHDx", https://ghdx.healthdata.org/gbd-results-tool. [accessed 25/03/2022].

[2] World Health Organization (2018) World Health Organization, *Global status report on road safety 2018: summary*. *World Health Organization*, Geneva.

[3] Kahane, C.J. and others (1986) National Highway Traffic Safety Administration, *An evaluation of child passenger safety: the effectiveness and benefits of safety seats: summary*, Washington D.C, USA.

[4] Rice, T.M. and Anderson, C.L. (2009) The effectiveness of child restraint systems for children aged 3 years or younger during motor vehicle collisions: 1996 to 2005. American Journal of Public Health, **99**(2): p.252–257.

[5] Economic Commission for Europe of the United Nations (UN/ECE) (2013) United Nations, *Regulation No 129 of the Economic Commission for Europe of the United Nations (UN/ECE) — Uniform provisions concerning the approval of enhanced Child Restraint Systems used on board of motor vehicles (ECRS)*. https://eur-lex.europa.eu/eli/reg/2014/129/oj. [accessed 25/03/2022].

[6] Thurn, C., Krebs, C., Visvikis, C., Kettner, M., and Xu, W. (2020) The effect of recline angle on upper neck force in UN Regulation No. 129 frontal impact tests of infant carries. *Proceedings of Conference Protection of Children in Cars Conference*, 2020, online.

[7] Stanford Children's Health (n.d.) "Infant Sleep", https://www.stanfordchildrens.org/en/topic/default?id=infant-sleep-90-P02237. [accessed 25/03/2022].

[8] Task Force on Sudden Infant Death Syndrome (2016) SIDS and other sleep-related infant deaths: updated 2016 recommendations for a safe infant sleeping environment. Pediatrics, **138**(5).

[9] Davis, N.L. and Shah, N. (2018) Use of car beds for infant travel: a review of the literature. Journal of Perinatology, **38**(10): p.1287–1294.

[10] Ratzek, A. (2018) Reclined infant carriers: Is there a gap in UN ECE Reg. 129? *Proceedings of Conference Protection of Children in Cars Conference*, 2018, Munich, Germany.

[11] Simcenter Madymo (2020) Siemens, *Mode Manual*. *Siemens Digital Industries Software*, The Hague, Netherlands.

[12] Gehre, C., Gades, H., and Wernicke, P. (2009) Objective rating of signals using test and simulation responses. *Proceedings of Conference International Technical Conference on the Enhanced Safety of Vehicles*, 2009, Stuttgart, Germany.

[13] Gehre, C. and Stahlschmidt, S. (2011) Assessment of dummy models by using objective rating methods. *Proceedings of Conference 22nd International Technical Conference on the Enhanced Safety of Vehicles Conference (ESV)*, 2011, Washington, D.C., USA.

[14] SAE (2007) SAE, *Instrumentation for impact test: Part 1 - electronic instrumentation compiled by SAE international*.

[15] Mertz, H.J., Irwin, A.L., and Prasad, P. (2003) Biomechanical and Scaling Bases for Frontal and Side Impact Injury Assessment Reference Values. Stapp Car Crash Journal, **47**: p.155–188.

[16] CLEPA (2020) United Nations, *UN R129: Proposal for the 04 series of amendments*, 68th GRSP, 07-11 December 2020 agenda item 12. https://unece.org/fileadmin/DAM/trans/doc/2020/wp29grsp/GRSP-68-05.pdf. [accessed 25/03/2022].

[17] Costandinos, V., Mark, P., Farid, B., Marianne, L.C., and Thomas, M. (2020) The development of pragmatic thresholds for upper neck tension force and flexion moment in Q-series dummies in UN Regulation N0. 129 tests. *Proceedings of Conference Protection of Children in Cars Conference*, 2020, online.

[18] Menon, R., Ghati, Y., and Jain, P. (2007) MADYMO simulation study to optimize the seating angles and belt positioning of high back booster seats. *Proceedings of Conference The 20th International Technical Conference on the Enhanced Safety of Vehicles (ESV)*, 2007, Lyon, France.

[19] Larsson, K.-J., Pipkorn, B., Iraeus, J., Forman, J., and Hu, J. (2021) Evaluation of a diverse population of morphed human body models for prediction of vehicle occupant crash kinematics. Computer Methods in Biomechanics and Biomedical Engineering.

Appendix

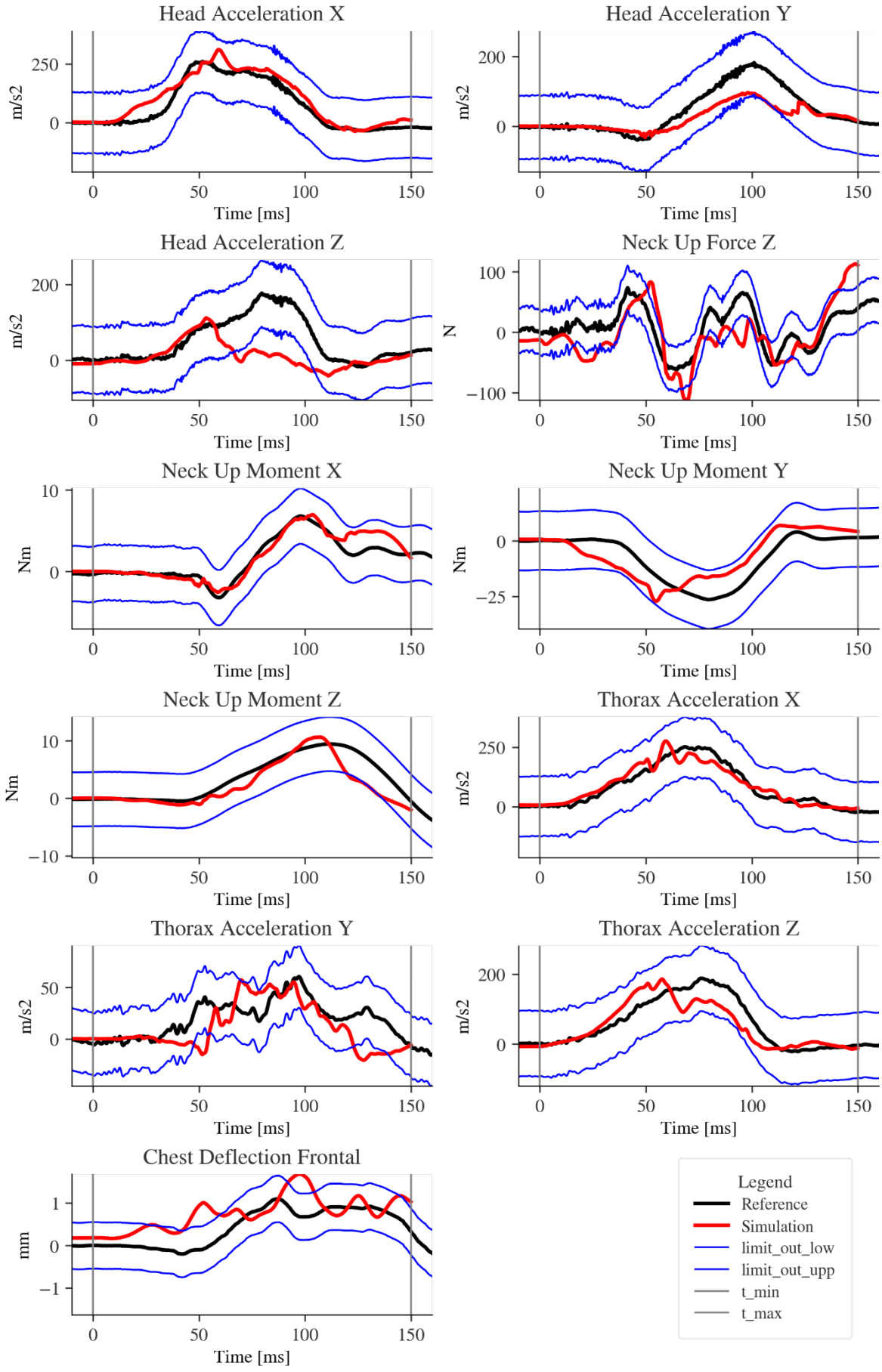

Figure 11. Signals used to calculate the CORA rating.

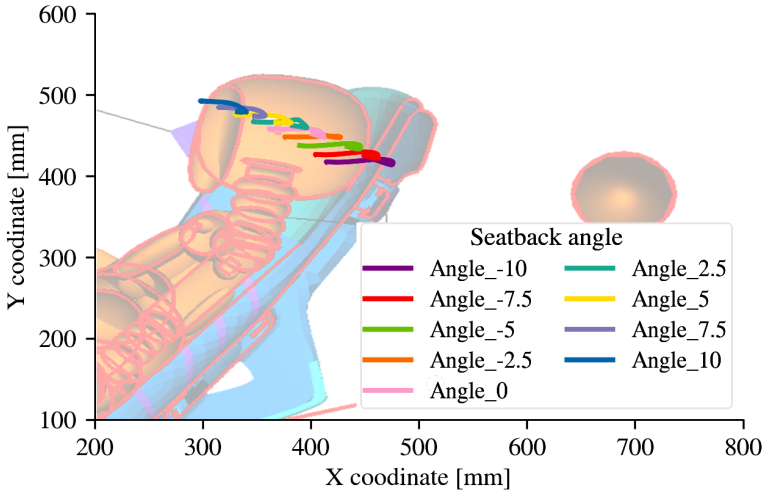

Figure 12. Head displacement in the sagittal plane for a CRS with different seatback angles.